Mechanistic aspects of glycerol oxidation on palladium electrocatalysts in model aqueous and fermentation media solutions

Y.E. Silina [a,*], E.V. Butyrskaya [b], M. Koch [c], C. Fink-Straube [c], N. Korkmaz [d], M.G. Levchenko [e], E.V. Zolotukhina [e,†]

[a] Institute of Biochemistry, Saarland University, Saarbrücken, Germany
[b] Department of Chemistry, Voronezh State University, Voronezh, Russia
[c] INM – Leibniz Institute for New Materials, Saarbrücken, Germany
[d] KIST Europe – Korea Institute of Science and Technology Europe Forschungsgesellschaft mbH, Campus E 7.1, D-66123, Saarbrücken, Germany
[e] Federal Research Center of Problems of Chemical Physics and Medicinal Chemistry, Russian Academy of Sciences, 142432 Chernogolovka, Moscow region, Russia

ARTICLE INFO

ABSTRACT

Herein, a study dealing with a progress on palladium (Pd) electrocatalysts for an efficient glycerol electrooxidation in model aqueous and real fermentation solutions with special focus on some physicochemical parameters (*e.g.*, the impact of adsorption stage of multiple species, presence of oxygen, influence of anodic limits and Pd-size) was conducted. During the course of investigations by tandem of an optical oxygen minisensor and cyclic voltammetry a significant impact of oxygen on the efficiency of glycerol electrooxidation on Pd electrocatalysts at alkaline pH in model aqueous and yeast fermentation media was revealed.

The obtained knowledge was used for the optimization of an assay utilizing Pd-sensing layers for glycerol determination and quantification in yeast fermentation medium. Received results showed a satisfactory agreement with a control measurement carried out by gas chromatography mass-spectrometry.

1. Introduction

Glycerol is a frequently used substrate for bacterial or yeast cells fermentation [1]. In some cases glycerol can be utilized as a signaling product of microbial activity of cells [2,3]. Therefore, the development of a rapid, simple in use, sensitive and selective measurement approaches enabling monitoring and control of glycerol in real biological samples would significantly assist our understanding on pathways of its production or conversion by cells.

Although several non-enzymatic amperometric assays based on noble metal-based electrodes (Au, Pt, Pd) applied for a rapid glycerol sensing in a variety of biological samples with different analytical merit were proposed [4]. However, the only a few attempts towards establishment of the mechanism underlying electrooxidation of glycerol or factors affecting the efficiency of the process were conducted [5]. At the same time, revealing and systematization of key aspects impacting glycerol electrooxidation could significantly promote the development of novel electrodes with a controlled design and tuned analytical properties.

The electrooxidation of glycerol undergoes the following route: sorbate adsorption (*1*), bond breaking and electron transfer (*2*), reaction between sorbate and adsorbed species on the surface (*3*) and product desorption (*4*) [6]. The intermediates formed during electrooxidation of glycerol on noble metals, in particular on Pd, were discussed in [6,7] in aspect of alkaline fuel cells. However, no attention has been paid to the chemical stages of glycerol and its intermediates alteration leading to the formation of electroactive species, *e.g.,* gem-diol forms of glyceraldehyde. At the same time, the key role of these species in the formation of an electrochemical signal for methanol and ethanol was proved [8,9]. Moreover, the electrochemical behavior of various types of Pd catalysts and experimental conditions of CV procedure used for the estimation of activity in glycerol oxidation reaction strongly differ from study to study that makes their comparison difficult (see **ESI, Table S1,** [10–16]).

The adsorption of glycerol (*1*) at alkaline pH on the surface of electrodes based on noble metals relies on the cleavage and transport of the hydrogen atom (the source of hydrogen could be $-CH_2$ or $-OH$ alcohol group) from the alcohol molecule retained on the surface of electrocatalysts [17–20]. Therefore, the use of electrocatalytic layers, *viz.*

---

palladium (Pd) which is known by its ability to support specific interactions with hydrogen, could enhance the cleavage of hydrogen and the overall oxidation efficiency of glycerol [21,22].

Although earlier it was shown that the adsorption of OH-species at alkaline supporting electrolytes can drastically affect the efficiency of alcohols electrooxidation on palladium electrodes [23], the fundamental reasons for this phenomenon remain non-understood. For example, why a concurrent adsorption of multiple species (*e.g.,* glycerol and hydroxyl) at the surface of the same electrode should assist the entire electrooxidation process is unclear [18,19,24]. More significantly, it was shown that the adsorption step of alcohols (*1*) on Pd is almost irrelevant in total electrochemical route [23].

Herein, the role of the oxygen released in alkaline media after hydroxyl decomposition on the surface of Pd-electrodes on glycerol electrooxidation efficiency was revealed. The obtained results open up the possibilities of a rational design of Pd-electrocatalytic layers based on the tuning of their surface properties for the efficient and controlled glycerol electrooxidation in model aqueous and real fermentation solutions.

2. Experimental part

2.1. Chemicals and materials

Graphene oxide and Pd-ink modified screen-printed electrodes (SPEs) were obtained from DropSens (Metrohm, Germany). H_2PdCl_4, $(NH_4)_2HPO_4$, $Na_2HPO_4 \cdot 12H_2O$, 25 % NH_4OH used to prepare a basic Pd-electrolyte (pH 9.1), glycerol solution (85 %), glyceric acid, KOH pellets, derivatization agent N-trimethylsilyl-N-methyl trifluoroacetamide (MSTFA), yeast fermentation HC complete medium (Hartwell's Complete medium) supplemented with 10 % of yeast nitrogen base (YNB) were received from Merck (Darmstadt, Germany).

2.2. Yeast fermentation

The received yeast colonies (*Saccharomyces cerevisiae* strain BY4742) were transferred to flasks filled with 10 mL of HC complete medium for a cultivation of 24 h The optical densities (OD) of the received yeast suspensions ranged from 3.0 ± 0.4 to 6 ± 0.3. After cultivation, cells were removed from the medium by centrifugation. The obtained medium after contact with cells was used for glycerol sensing. Prior to electrochemical studies, the pH of the model aqueous and fermentation (collected surfactants) samples was set to 12 using KOH pellets.

2.3. Formation of functional layers of electrodes and electrochemical studies

Herein, several designs of electrodes modified by Pd electrocatalysts (*e.g.,* Pd-ink (*i*), Pd-nanoparticles (Pd-NPs) (*ii*) and hybrid Pd-ink/Pd-NPs (*iii*) layers) were explored towards glycerol electrooxidation.

Pd-ink modified SPEs were used in their original form. To compare the electrocatalytic performance of Pd-ink electrodes towards glycerol electrooxidation, SPEs modified by Pd-nanoparticles (Pd-NPs) were utilized. Pd-NPs were formed on the surface of commercial SPEs modified by graphene oxide (GO) during galvanostatic deposition at a cathodic current of -2.5 mA (current density was 19.9 mA cm^{-2}) for 30 s from the alkaline electrolyte (pH 9.1) according to a previously reported protocol [25]. The used polarization mode leads to Pd deposition from the solution accompanied by a hydrogen evolution reaction. These conditions enable to avoid the multicycle CV activation of the metal surface in the range of hydrogen adsorption/desorption potentials.

To compare the commercial Pd-ink modified and homemade Pd-NPs, it was proposed to synthesize an electrode with a hybrid functional Pd-layer. For this goal, Pd-NPs were deposited at the same electrochemical parameters (*i.e.* cathodic current of -2.5 mA for 30 s) from the same basic electrolyte (pH 9.1) on a Pd-ink surface (hybrid Pd-ink/Pd-NPs).

The estimation of the electroactive surface area (ECSA) of Pd electrocatalysts was performed *via* CO electrodesorption method in a three-electrode electrochemical cell and by oxygen desorption method according to a previous study [9]. The specific ECSA value was calculated by the use of Pd weight estimated by Faraday's law from the charge passed during dissolution of Pd from the electrode in 1 M HCl. The dissolution of the palladium layer from SPEs was conducted in a galvanostatic mode at 0.1 mA for Pd-NPs and 0.5 mA for Pd-ink and hybrid electrode.

The electrochemical measurements were carried out in three-electrode electrochemical cell (equipped with Schlenk line to maintain an argon, air or CO atmosphere) with a Pt wire counter electrode and silver chloride or Hg/HgO, OH$^-$ reference electrodes (depending on the solution composition) separated from the working solution by a double frit. In these experiments, the SPE working electrode was connected to the signal input of the PGstat *via* a special plug. The solution volume was 15 mL in these experiments. The applied level of pH was defined for glycerol electrooxidation in our previous study [26].

In other series of experiments the Pd modified SPEs was explored in a droplet mode at ambient conditions (open system). Ag/Ag$_2$O, OH$^-$ reference electrode of SPE and carbon counter electrode of SPE were used in this set of experiments. The studied electrolyte was placed on the surface of SPE and fixed in the connector box of the potentiostat (PalmSens4, Utrecht, The Netherlands). The 0.02 M KOH, pH 12 or potassium phosphate buffer, pH 7 were used as electrolytes. For the electrochemical experiments the volume of the electrolyte droplet was 150 μL.

The comparison of electrochemical activity of studied electrodes was carried out by the use of two approaches, *e.g.,* by external standard calibration, ESTD, used for model glycerol solutions and by multiple standard addition approach applied for real fermentation medium.

2.4. Scanning electron microscopy (SEM/EDX)

The morphology of SPEs was studied by scanning electron microscopy (SEM) in high vacuum mode on a FEI (Hillsboro, OR, USA) Quanta 400 FEG system equipped with an EDAX (Mahwah, NJ, USA) Genesis V 6.04 X-ray module at a voltage of 10 keV.

2.5. Atomic force microscopy (AFM)

AFM topography measurements of the samples were performed using a NX 10 AFM system (Park Systems, Korea) using noncontact mode under ambient pressure and at room temperature. Pre-mounted ACTA-10 probes ("material: Si, N-type, 0.01–0.025 ohm/cm", cantilever length (L): 125 μm, width (W): 30 μm, thickness (T): 4 μm, tip-radius: <10 nm, frequency (f): 200–400 kHz, spring constant (k): 13–77 N/m, coating: Al (reflex side)) were purchased from AppNano (USA). Topography images (scan size of 25 μm x 25 μm) were recorded with a resolution of 256 pxl x 256 pxl. Imaging settings were automatically set by the Park SmartScan™ operating program and AFM data were further processed with the free Gwyddion software including 3D image re-construction. For data acquisition, two roughness parameters, namely arithmetic average roughness (R_a) and root mean square roughness (R_q) values were obtained using Gwyddion software for four 25 μm x 25 μm images for each sample. Roughness was presented as mean R_a and R_q values ±SD.

2.6. Oxygen minisensor studies

To evaluate the intensity of oxygen consumption or release at Pd-electrocatalysts, the oxygen concentration (μmol·L^{-1}) in a droplet of test solutions was monitored by an OXR430 needle oxygen minisensor (Pyro Science GmbH, Aachen, Germany). The calibration of the minisensor prior to use was performed in accordance with manual recommendations in air (*1*) and in a test-liquid (*2*). During recording of the

oxygen consumption values the electrodes were operated in CV mode in the range of −0.4 …0.8 V (unless otherwise stated).

2.7. Quantum-chemical calculations

To study the impact of the adsorption stage on glycerol electro-oxidation at Pd-electrodes, quantum-chemical studies were carried out using density functional theory (DFT) B3LYP.[11] The 6–31G(d,p) basis set was utilized for O, N, H atoms [27]. For Pd, a LANL2DZ ECP basis with added f-polarization function was applied [28,29].

During the calculations, the position of glycerol was varied on the surfaces of Pd and PdO fragments. The Gibbs (G_{ads}) and total (E_{ads}) adsorption energies of glycerol on Pd (PdO) clusters were calculated as follows:

$$G_{ads} = G_{12} - (G_1 + G_2) \qquad (1)$$

$$E_{ads} = E_{12} - (E_1 + E_2) \qquad (2)$$

where G_1 and G_2 – are the Gibbs energies of fragments 1 and 2, G_{12} – is the Gibbs energy of the system obtained by combining of these fragments into a complex; E_1 and E_2 – are the total energies of fragments 1 and 2, E_{12} – is the total energy of the system obtained by combining of these fragments into a complex.

So far, the electrooxidation of glycerol was studied on Pd-based electrodes at pH 12, the calculations were also performed for hydroxyl radical, OH [23].

2.8. Gas-chromatography mass spectrometry (GC–MS)

For quantitative analysis of glycerol in yeast fermentation samples, a previously published protocol utilizing standard additions was used [26]. Briefly, fermentation samples were derivatized with MSTFA at 60 °C for 30 min followed by a subsequent GC–MS separation performed on a QP5050 GC–MS system (Shimadzu, Japan) equipped with a PAL auto sampler (CTC Analytics, Zwingen, Switzerland). For this goal, 0.5 μL of the derivatized sample was injected into the system. A ZB-5HT Inferno column (30 m × 0.25 mm, thickness 0.25 μm) was used in GC–MS experiments: start temperature 50 °C held for 2 min, raised to 300 °C at 25

K/min and held at 300 °C for 1 min. Mass spectra were recorded in TIC and SIM modes in the range of m/z 100 – 500. MS interface was set at 250 °C, ion source temperature was 200 °C.

3. Results and discussion

3.1. Comparison of morphology, composition and electrochemical activity of Pd-electrodes in glycerol oxidation reaction

Three types of SPEs were used in this study: (*i*) Pd-NPs modified electrodes, where the functional layer was formed *via* electrodeposition of Pd from the solution on the surface of the working electrode, (*ii*) commercial Pd-ink SPE and (*iii*) a hybrid electrode based on a commercial Pd-ink with electrodeposited Pd-NPs (will be further refereed to Pd-ink/Pd-NPs).

EDX spectra recorded from the studied Pd-electrocatalysts (*i-iii*) indicate the increase of Pd-mass/counts for the hybrid Pd-ink/Pd-NPs layer as compared to the individual Pd-ink or Pd-NPs (**Fig. S1**). This result was confirmed by SEM studies: thus, the pronounced difference in the morphology of electrocatalytic layers was seen with an obvious visual increase of Pd-deposits amount for the hybrid Pd-ink/Pd-NPs layer, Fig. 1**A-C**.

The Pd-ink functional layer was represented by spheres with an average diameter of 600 – 800 nm partially covered by polymer (Fig. 1**A**). The Pd-NPs layer consisted of much smaller nanoparticles (NPs) with a diameter of 40 – 60 nm (Fig. 1**B**). Remarkably, Pd-NPs deposited on Pd-ink (Pd-ink/Pd-NPs hybrid) at the same current and time as it was used for Pd-NPs synthesis were larger in diameter, *i.e.* 600 – 800 μm *vs* Pd-NPs formed on an empty electrode (graphene oxide-modified SPEs), *e.g.,* 40 – 60 nm, Fig. 1**C**. This phenomenon can be explained by the deposition and growth of Pd particles on polymer-free parts of the Pd-ink surface. It was in accordance with a known observation: the type of the surface/template significantly determines the morphology of electroplated Pd-deposits [30].

Subsequently, performed investigations of the topography of the electrodes supported the obtained SEM/EDX results: although no pronounced topographical changes were detected by AFM studies for Pd-ink (Fig. 1**D**) and hybrid Pd-ink/Pd-NPs modified electrodes (Fig. 1**F**), the
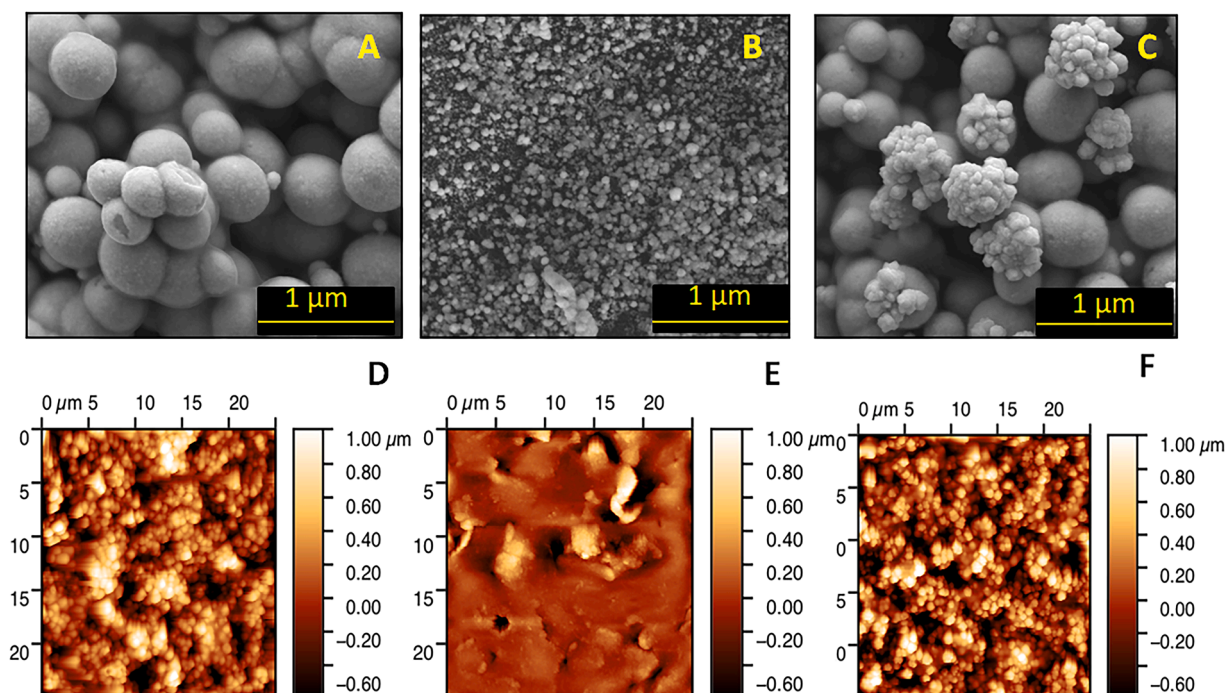
Fig. 1. SEM (**A-C**) and AFM (**D-F**) topography images of Pd-modified SPEs: (**A,D**) – Pd-ink; (**B,E**) – Pd-NPs; (**C,F**) – hybrid Pd-ink/Pd-NPs layer.

calculated values of the average roughness (R_a) and surface root mean square roughness (R_q) clearly showed a significant enhancement for the hybrid Pd-layer, **ESI, Fig. S2**.

The comparison of SEM/AFM data with the determined ECSA values summarized in Table 1 allows to conclude that the ECSA found for the hybrid electrode is mostly provided by additionally deposited Pd-NPs, that could be explained by the composition and morphology of the commercial Pd-ink electrode. The surface of the commercial Pd-ink electrode consisted of agglomerates of spherical Pd-nanoparticles surrounded by a thin isolating polymer film [26]. The absence of the gain in Pd weight for the hybrid modified electrode in comparison to the Pd-ink electrode can be explained by a partial loss of Pd from the Pd-ink layer due to the associated hydrogen evolution process.

The electrochemical responses for the studied Pd-modified SPEs in a full polarization range −0.4 … 0.8 V in model glycerol solutions were similar, *viz.* there are two anodic waves corresponded to glycerol oxidation marked on curves in Fig. 2 as A_1 at −0.1 V and A_2 with the onset potential at about 0.4 V. The latter wave appeared in the range corresponding to Pd electrooxidation in a background solution. At the same time, the anodic current responses recorded from Pd electrocatalysts in the potential range −0.4 … 0.8 V increased from cycle to cycle (**Fig. S4, ESI**). Notably, this trend was more pronounced for Pd-NPs modified electrode: the peak A_1 at −0.1 V was absent in the first cycle of CV; however, starting from the second scan the main anodic peak corresponding to glycerol electrooxidation was recorded. A restriction of the cathodic limit (except for the hydrogen adsorption/ desorption region) is necessary to exclude the influence of electrode pH changes accompanied with changes of composition of electroactive species near the electrode surface. The influence of the cathodic polarization limit on current responses was described in [9]. Surprisingly, the current densities (calculated from ECSA) of these peaks changed independently on ECSA of studied electrodes, *viz.* the current densities found for Pd-NPs-modified SPE were comparable with hybrid-modified SPE, while the ECSA and specific ECSA (SECSA) of these electrodes were different (Table 1). The obtained analytical merit (*e.g.,* LDR, sensitivity) of the tested Pd electrodes in model glycerol solutions was in line with results reported in literature [12,31–36].

Comparison of current responses of Pd-ink and Pd-hybrid modified SPEs also demonstrated the inconsequent activity in glycerol oxidation reaction, *viz.* the hybrid electrode with lower ECSA and specific ECSA demonstrated the highest responses. Moreover, the sensitivity of studied electrodes to glycerol in model solutions in the same linear dynamic range (LDR), 1–100 mM, estimated from CV at potential of wave A_2, 0.55 V, varied independently on ECSA values. That was unexpected, because the difference in the morphology and ECSA of electrodes is usually the main reason for their different electrochemical activity, given the same nature and composition of electrocatalyst.

The diminution of the anodic polarization limit to 0.6 V led to a current decrease in the anodic branch of CVs corresponding to glycerol oxidation for both Pd-ink modified SPE and a hybrid electrode (Fig. 2). Pd-NPs modified electrode didn't show any anodic response corresponding to glycerol oxidation in the reduced anodic range. This electrochemical behavior indicates that the anodic processes occurring on Pd-surface at potentials higher than 0.4 – 0.6 V are necessary for an

efficient glycerol oxidation.

The influence of pH on the glycerol electrooxidation was typical for alcohol oxidation reactions on Pd, *i.e.* the increase of pH leads to an increase of the current responses on the anodic branch of CVs (**ESI, Fig. S5**).

To sum it up, some features of glycerol electrochemical oxidation on the surface of various types of the studied Pd electrodes could be highlighted, *viz.* independence of electrochemical activity on ECSA and the influence of the anodic polarization limit on electrochemical activity of electrodes.

Keeping in mind the complex mechanism of alcohols electrooxidation including formation of several intermediates and participation of oxygenic species [37,38], the influence of the adsorption stage of oxygen on Pd particles could be the main reason for the observed electrochemical features of studied electrodes. The impact of oxygenic species and preliminary chemical stages on the activity of Pd-modified electrodes in methanol and ethanol oxidation reactions was in detail discussed in previous works [8,9,39]. For glycerol oxidation reaction, the experiment with a preliminary polarization-less keeping of electrode in alcohol solution described in [8] was repeated here as an additional argument supporting the influence of oxygen on the process. From Fig. 3 it is seen that the preliminary keeping of electrodes in a contact with the analyzed glycerol solution during only 10 min without polarization leads to an increase and stabilization of the current responses on CV.

At the same time, the electrochemical behavior of glyceric acid at pH 12 on the same Pd-electrode is different (Fig. 3, curve *5*) from glycerol. Thus, the oxidation peak of glyceric acid was shifted to a more negative potential (−0.2 V) and CV responses remained constant from cycle to cycle (no changes were recorded for glyceric acid *vs* glycerol). It means that the preliminary chemical stages occurred on the surface of Pd in a glycerol solution lead to the formation of an electroactive product subsequently adsorbed and electrochemically transformed on the electrode surface.

Next, to clarify and systemize the key parameters (*e.g.* adsorption) affecting glycerol electrooxidation on the surface of palladium electrocatalysts in alkaline medium, quantum-chemical simulations were conducted (*see next section*).

3.2. Quantum-chemical calculations of glycerol adsorption in dependence on the oxygenic species presence on Pd surface

The overall reaction of glycerol electrooxidation in an alkaline medium can be described as follows [40]:

$$CH_2OH—CHOH—CH_2OH + 20OH^- \rightarrow 3CO_3^{2-} + 14H_2O + 14\bar{e} \quad (3)$$
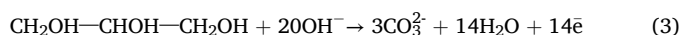
The reaction (3) proceeds in several steps resulting in the formation of intermediates having substantially less activation energy. Most authors believe that the initial stage underlying glycerol electrooxidation starts with a cleavage of hydrogen atom from CH_2^- or OH-group of glycerol [6,25]. However, hydroxyl-ions present in solution at pH 12 can also be adsorbed on the surface of Pd electrode. As it is seen from Fig. 4A,B, the change of Gibbs' energy, G_{ads}, during adsorption of hydroxide ions on the Pd-surface was negative while in the case of glycerol,

Table 1.
Evaluation of ECSA and activity of Pd-based electrodes in glycerol oxidation reaction.

System	ECSA, cm^2	Pd weight, μg	SECSA, m^2/g	SA (A_1), μA·cm^{-2} *	SA(A_2), μA cm^{-2}	MA(A_2), μA μg^{-1}	Sensitivity**, μA mM^{-1} cm^{-2}	LDR***, mM
Pd-NPs	2.0	6.5 ± 0.5	31	266	273	85	0.77	1 – 100
Pd-ink	9.2	257±24	3.6	68	75	2.7	0.58	1 – 100
Hybrid (Pd-ink/Pd-NPs)	4.9	243±26	2.0	237	169	3.4	1.51	1 – 100

* SA – surface activity, *i.e.* the peak current to ESCA ratio, MA – mass activity;.

** read-out to glycerol at 0.6 V; sensitivity to glycerol was evaluated in model solutions in the concentration range of 1–100 mM;.

*** linear dynamic range evaluated by external standard (ESTD) approach in model glycerol solutions, see also **ESI, Fig. S3**.
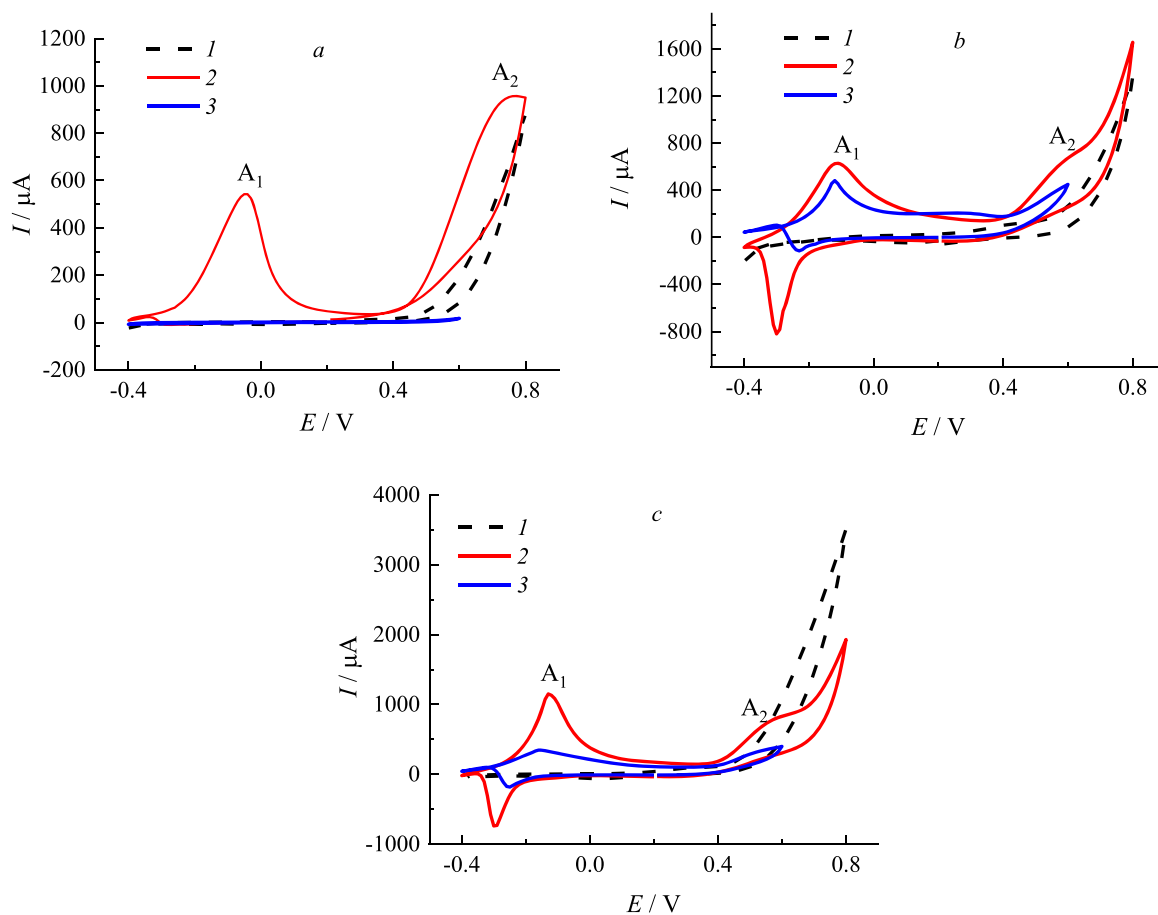
Fig. 2. CV curves recorded from SPEs modified with (*a*) Pd-NPs, (*b*) Pd-ink and (*c*) hybrid Pd-NPs/Pd-ink layer in (*1*) 0.02 M KOH and (*2,3*) in the same background electrolyte supplemented with 100 mM glycerol in various polarization ranges: −0.4 … 0.8 V (*1,2*), −0.4 … 0.6 V (*3*). Scan rate 20 mV/s, 3rd cycles shown, all potentials given *vs.* Ag/Ag$_2$O electrode.
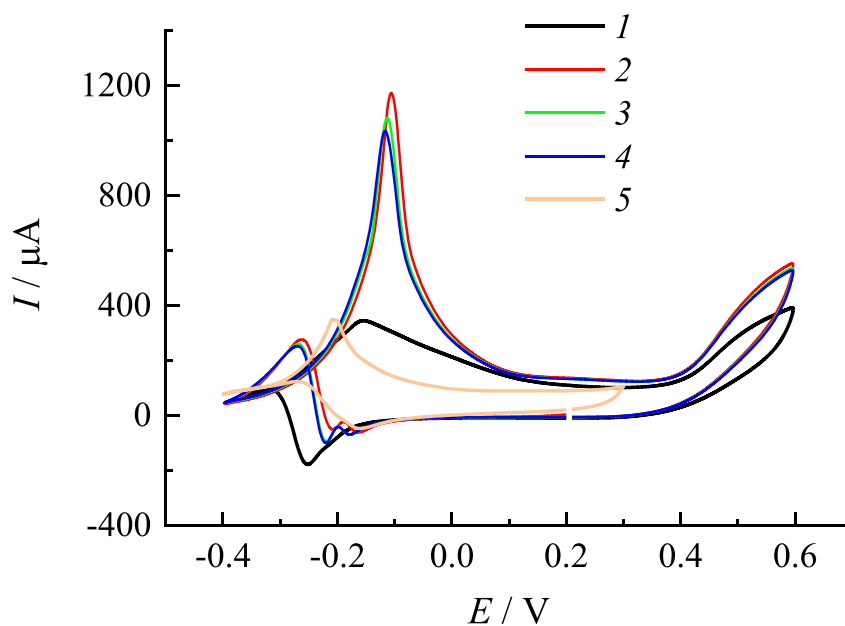
Fig. 3. CV curves of Pd-ink modified SPE in (*1–4*) 100 mM glycerol or (*5*) 100 mM glyceric acid solution pH 12. *1, 5* – 3rd cycle of CV registered immediately after contact with solution, *2–4* – 1st −3rd cycles of CV correspondingly recorded after 10 min of contact of the electrode with solution (without polarization). Scan rate 20 mV/s, all potentials given *vs.* Ag/Ag$_2$O electrode.

OH⁻ anion on Pd-based electrode **A**   Glycerol on Pd-based electrode **B**

E_{ads} = -148.75 kcal/mol

G_{ads} = -100.79 kcal/mol

E_{ads} = -16.32 kcal/mol

G_{ads} = 32.62 kcal/mol

OH⁻ anion on PdO-based electrode **C**   Glycerol on PdO-based electrode **D**

E_{ads} = -121.95 kcal/mol

G_{ads} = -109.37 kcal/mol

E_{ads} = -21.79 kcal/mol

G_{ads} = -7.55 kcal/mol
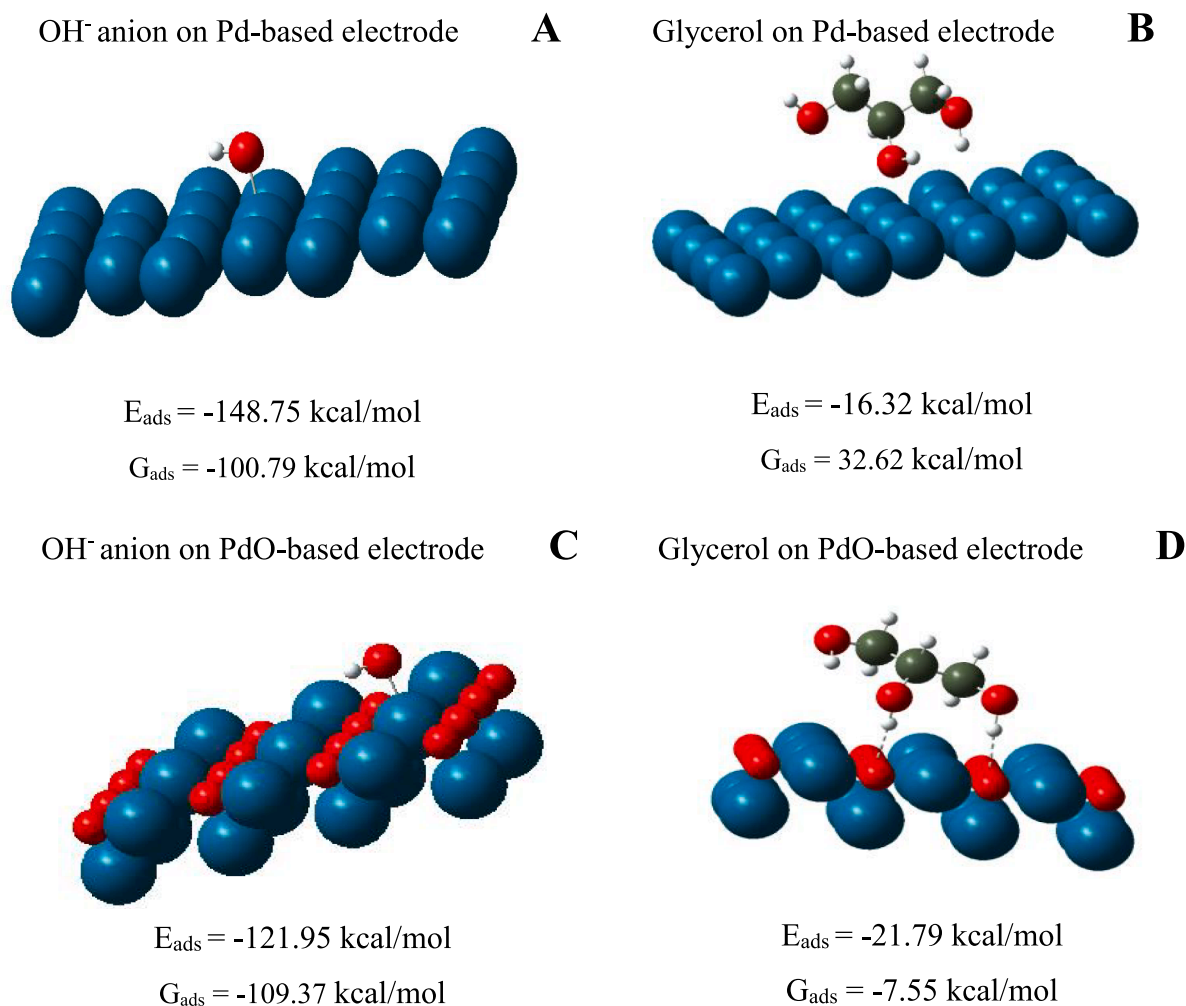
Fig. 4. The most advantageous location of glycerol (**B, D**) and hydroxyl (**A, C**) on Pd (**A, B**) and PdO (**C, D**) surfaces.

the positive changes of Gibbs' energy indicates a non-spontaneous process. In contrast, on the surface of PdO the adsorption of glycerol leads to a diminution of Gibbs' energy (Fig. 4,**D**) *vs* oxides-free Pd-surface. At the same time, the adsorption of hydroxyls ions on both Pd and PdO is advantageous compared to glycerol.

Glycerol is a weak acid, pK_a 14.4 [41], and the detachment of the first proton leads to its electrochemical transformation to glyceraldehyde or ketone (Fig. 5). Its hydration leads to the formation of carbonyl or keto-group to a gem-diol form [42,43] which could be further transformed in the presence of OH-ions to a gem-diolate anionic form. These chemical transformation stages are known from literature, however, hardly discussed in terms of the mechanism of glycerol oxidation and factors affecting this process [6,43,44], see also refs. in **Table S1**.

The optimized gem-diol forms of glyceraldehyde possibly formed in

an aqueous solution on both Pd and PdO surfaces are summarized in **Table S2, ESI**. As it can be seen the G3 and G4 structures are transformed on Pd surfaces. Moreover, the G3 structure is unstable on the Pd surface and loses one hydroxyl group, whereas on the PdO surface this form is more stable compared to the solution. The estimation of Gibbs energy changes during adsorption of various gem-diol forms on Pd showed the negative values only for the transformed G4 structure. In contrast, the adsorption of G1-G5 structures on PdO surface leads to the diminution of Gibbs energy, while the adsorption of G2 and G4 structures is more favorable. All structures were tested for their stability by frequency analysis. During analysis the absence of imaginary frequencies in these structures was established that confirmed their stability and correspondence not to transition states, but to minimum on the potential energy surface.
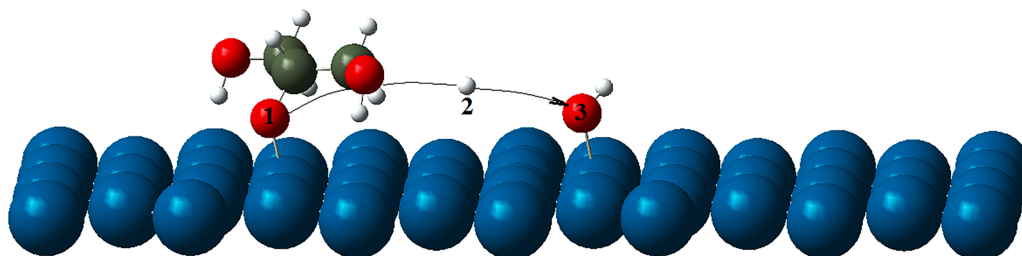
Fig. 5. Transfer of the hydrogen atom *2*, initially bound to the central oxygen atom of glycerol *1* to the oxygen atom *3* of the adsorbed hydroxyl anion resulting in H_2O formation ($H^+ + OH^- = H_2O$), blue – Pd, red – O, white – H.

The obtained data confirmed that the adsorption of gem-diol forms is more favorable even on Pd surface in comparison with glycerol. It is hypothesized, that the first oxidation peak at -0.1 V corresponds to the oxidation of gem-diolate form of glyceraldehyde, by analogy of acetaldehyde or formaldehyde gem-diolates previously described in [9]. Hence, the transformation of this peak in CV mode and current increase from scan to scan in the absence of electrode polarization during 10 min (**Fig. 3**, see also **ESI, Fig. S3**) could be explained *via* a slow formation of electroactive gem-diolate species oxidized at -0.1 V on the electrode surface.

Notably, the diminution of Gibbs energy during adsorption of OH-ions or glycerol (gem-diol) on palladium modified by oxygenic species preliminary highlights the role of oxygen on the efficiency of glycerol electrooxidation. It should be mentioned that not only the intact surface chemistry of Pd-electrodes can serve as a source of oxygenic species, but also previously adsorbed OH-ions. Thus, OH-ions can readily be decomposed on a Pd-surface according to the following sequence [45]:

$$2OH_{ads}^{-} \rightarrow H_2O_{ads} + O_{ads} + 2\bar{e} \tag{4}$$

$$O_{ads} + O_{ads} \rightarrow O_{2ads} \rightarrow O_2 \tag{5}$$

As a result of the decomposition of OH-groups, the overproduction of oxygen in test-solutions can be expected in a specific range of potentials. To verify this assumption, next, the luminescent oxygen minisensor was used during electrochemical measurements with glycerol.

3.3. Electrochemical «detailing» of oxygen participation in glycerol electrooxidation

The optical oxygen minisensor measures the luminescent response of its active sensing layer in dependence on the concentration of the dissolved oxygen in solution [46]. Thus, the synchronization of the response of a minisensor with CV-responses in time would enable to evaluate the evolution/consumption of the dissolved oxygen even in the open system (ambient conditions).

To test the proposed set-up, firstly, the electrochemical behavior of Pd-modified electrodes was compared in model solutions at pH 7 and pH 12. The current-time (from 3$^{\mathrm{d}}$ CV-cycles) and oxygen concentration-time diagrams were combined in one image. The results are summarized in **Fig. S6 (ESI)**.

Briefly, for all studied Pd-modified electrodes in model glycerol solutions clear oxygen consumption in the cathodic wave of CV was observed followed by oxygen evolution during the anodic peak. The "saturation" of the oxygen minisenor response in a solution at pH 12 correlates well with the facilitation of oxygen evolution in alkaline media during the anodic polarization in comparison with neutral pH.

Interestingly, in glycerol solutions at pH 12, the oxygen minisensor response changes depending on the anodic polarization limit of CV curves. Thus, the oxygen consumption increases in the presence of glycerol during the cathodic polarization and oxygen release occurs in a solution only when the polarization reaches a value higher than 0.6 V, **Fig. 6**.

Moreover, the diminution of oxygen release from cycle to cycle of CV was seen even if the polarization anodic limit achieves 0.8 V (**Fig. 6a**). Diminution of the anodic limit to 0.6 V leads to significant changes in the response of the oxygen minisensor (**Fig. 6b**). In latter case, the overall concentration of oxygen in solution is diminished from the 1st cycle of CV to the last scan and a slight release of oxygen during the anodic polarization did not compensate the diminution of its overall concentration. In addition, the current responses corresponded to glycerol oxidation at -0.1 V diminished with a restriction of the polarization limit to 0.6 V.

Both oxygen minisensor and current CV responses recorded from the hybrid Pd-NPs/Pd-ink modified electrode demonstrated a similar behavior with the restriction of the anodic polarization limit (**ESI, Fig. 7b,c**). On the contrary, for Pd-NPs modified electrode, both responses were quite different, *i.e.*, even in the case of an extended polarization range ($-0.4 \ldots 0.8$ V) a great oxygen consumption was observed during 3 cycles of CV (**ESI, Fig. S7c**). The oxygen release occurred only during the first cycle of CV where the current response at -0.1 V corresponded to glycerol oxidation was absent. The subsequent restriction of the polarization limit to 0.6 V resulted in the absolute inactivation of Pd-NPs modified SPE to glycerol oxidation (**ESI, Fig. S7d**).

Experiments performed in a three-electrode electrochemical cell under argon atmosphere confirmed that the presence of dissolved oxygen facilitates the oxidation of glycerol. The increase of the anodic limit during polarization or replacement of the inert atmosphere to air leads to the increase of anodic currents corresponding to glycerol oxidation (**Fig. S8, ESI**). However, due to the large solution volume in comparison to the electrode surface in a standard cell the effect of oxygen influence is less pronounced *vs.* measurements conducted in a droplet mode with a thin layer of electrolyte on the electrode surface.

The above-made observations affecting glycerol oxidation on Pd electrocatalysts during the anodic polarization can be summarized as follows: (*i*) reduction of the anodic limit in CV leads to a decrease of the anodic current responses during glycerol oxidation; (*ii*) the impact of oxygenic species on glycerol oxidation in alkaline medium differs depending on the size of Pd-electrocatalysts (oxygen consumption in the presence of glycerol was seen for Pd-NPs modified electrode which should be the most active because of a size effect; in contrast, for Pd-ink as well as for the hybrid Pd-NPs/Pd-ink modified SPEs a significant
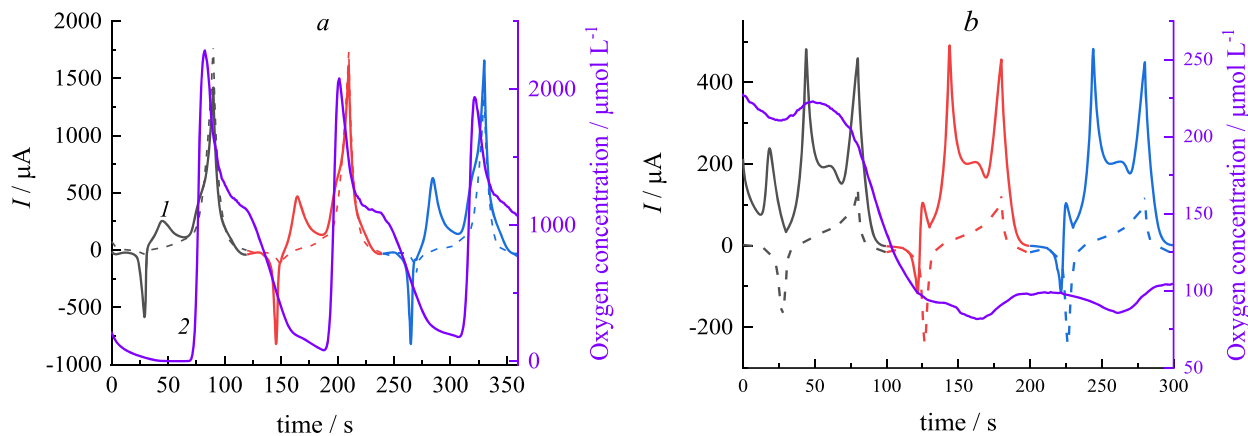
Fig. 6. Overlaid oxygen electrochemical responses recorded from Pd-ink modified SPE during CV (*1*) and results of simultaneous oxygen minisensor measurements (*2*) in 0.02 M KOH +100 mM glycerol. Polarization limit: (*a*) – 0.8 V, (*b*) – 0.6 V. Scan rate 20 mV/s. *Note*: various colors of curve *1* indicates the different cycles of CV (1st, 2nd, 3rd); dashed lines – current responses in the background solution at pH 12 (in the absence of glycerol).

oxygen release was recorded); (*iii*) the absence of the electrochemical response to glycerol on Pd-NPs without an additional source of oxygen provided by the extended anodic polarization limit.

It can be assumed, that Pd-electrodes with large particles (Pd-ink or hybrid Pd-NPs/Pd-ink layers) demonstrating weak interactions with oxygenic species could be more active in glycerol oxidation reaction. To prove this statement, the electrode modified with large Pd particles was synthesized *via* electrodeposition approach. The electroanalytical merit of this electrode was further compared with the electrode modified with small Pd-NPs in the glycerol oxidation reaction (*see next section*).

3.4. Impact of synthesis parameters of Pd-NPs on glycerol electrooxidation

Next, large Pd particles were formed on SPEs by extending the deposition time to 120 s and applying a cathodic current of −6 mA. The increase of Pd-NPs size (−2.5 mA for 30 s) from 40 – 60 nm to 500 – 1000 nm (−6.0 mA for 120 s, Fig. 7, SEM data) has led to a significant increase of the anodic current densities in glycerol solution (Fig. 7, CV curves). It should be mentioned, that these two electrodes differ only by the electrodeposited Pd weight and ECSA and the possible impact of the electrode support can be excluded. For Pd-NPs electrodeposited at −6 mA, 120 s the ECSA was 1.2 cm^2, the weight estimated from electrolytic dissolution of Pd was 16.5 $\pm$ 0.9 μg, SECSA 7.2 m^2/g. Moreover, this model experiment confirmed the above-made hypothesis: the larger Pd-particles better catalyze glycerol oxidation due to a weaker interaction with oxygen.

This result was in line with the oxygen mini-sensor behavior. In comparison to the small electrodeposited Pd-NPs (−2.5 mA, 30 s), the dynamic response recorded from the electrode modified by larger Pd-NPs (−6 mA, 120 s) was different, **ESI, Fig. S9**. Thus, a strong oxygen consumption was seen in the entire scanning range on small Pd-NPs (produced at −2.5 mA, 30 s) *vs* larger Pd-NPs (formed at −6 mA, 120 s). Briefly, the release of oxygen was observed during the entire scanning. Moreover, the concentration of the dissolved oxygen in solution slightly increased from cycle to cycle of CV. In other words, the increase of oxygen release for the electrode modified by larger Pd-NPs (−6 mA, 120 s) promotes the glycerol oxidation reaction. To facilitate glycerol oxidation, the increase of the oxygen content in a thin layer of electrolyte by an extension of the anodic polarization limit to potentials corresponding to oxygen release can be applied.

3.5. Impact of medium on glycerol electrooxidation at alkaline conditions

In the next set of experiments using oxygen minisensor and yeast

fermentation medium taken after pH correction (pH 12), no free dissolved oxygen was detected in these samples regardless of the used anodic limit, Fig. 8a,b. The absence of the dissolved oxygen in yeast fermentation medium was also confirmed in the absence of polarization (oxygen concentration was found at a level of 1 – 3 μmol/L). This result can be explained by a strong oxygen consumption necessary to support the chemical oxidation of components of the media (carbohydrates, amino acids, etc.) occurring at alkaline pH [47–50]. In this regard, the anodic signal related to glycerol oxidation at Pd electrocatalysts in HC medium (pH 12) can readily be suppressed or even absent. Indeed, the weak anodic waves at 0 V and 0.65 V appeared on CV (**Fig. S10a, ESI**) only in case of an extended anodic polarization (0.8 V), whereas at a restricted polarization (anodic limit 0.6 V), the current responses in HC medium in the presence or absence of glycerol were practically equal (Fig. 8b).

In addition, the anodic current response in the extended polarization range was reduced almost in 3.6 times as compared to model glycerol solutions (see Fig. 6a). The diminution of the current response corresponded to glycerol oxidation in HC medium correlates well with data recorded in a standard cell under inert atmosphere (**Fig. S8a, ESI**). It means that the deficit of the dissolved oxygen suppresses the glycerol electrooxidation on Pd electrocatalysts at alkaline pH. The obtained results highlight the sufficient role of molecular oxygen presence and impact of the media on glycerol electrooxidation on Pd.

3.6. Electroanalytical performance of Pd-electrodes in real yeast fermentation medium

Finally, the electroanalytical performance of Pd-ink, Pd-NPs and hybrid Pd-ink/Pd-NPs SPEs was quantitatively evaluated in HC fermentation medium collected after cultivation of yeasts. For this goal, the multiple standard addition approach of glycerol solutions of variable volume was used. This approach enables to overcome the matrix effects [51-53]. Concisely, by skipping of HC medium taken after 24 h of yeasts cultivation, it was revealed that an average glycerol content was 60.16 $\pm$5.3 mM, Table 2. The recovery for glycerol utilizing Pd-ink modified electrode was ranged from 94 % to 105 %; for Pd-NPs-based electrode – from 100 % to 112 %; for the hybrid Pd-ink/Pd-NPs – from 98 % to 103 %, respectively.

As expected, the highest sensitivity in real fermentation samples (HC medium) was detected for the hybrid Pd-ink/Pd-NPs electrode, the lowest – for Pd-NPs-based electrode. The obtained trends in medium were in line with those seen in model solutions (Table 1), however, with less intensity and efficiency: the highest glycerol electrooxidation efficiency in alkaline media was observed on the large Pd-structures than
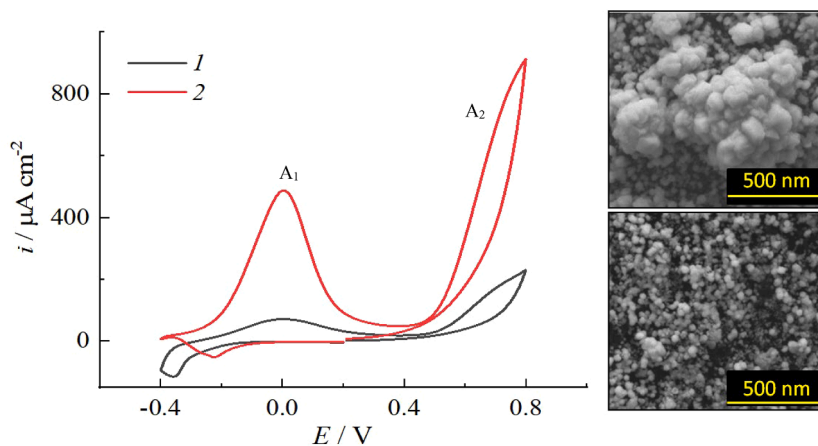
Fig. 7. CV plots of Pd-NPs modified SPE recorded in model glycerol solutions at pH 12: *1* – Pd-NPs were synthesized at −2.5 mA for 30 s; *2* – Pd-NPs were synthesized at −6 mA for 120 s and corresponding SEM images of the functional Pd-layers (electrode surface). *Note:* scan rate 20 mV/s, 3rd scans shown, all potentials given *vs.* Ag/Ag₂O electrode.
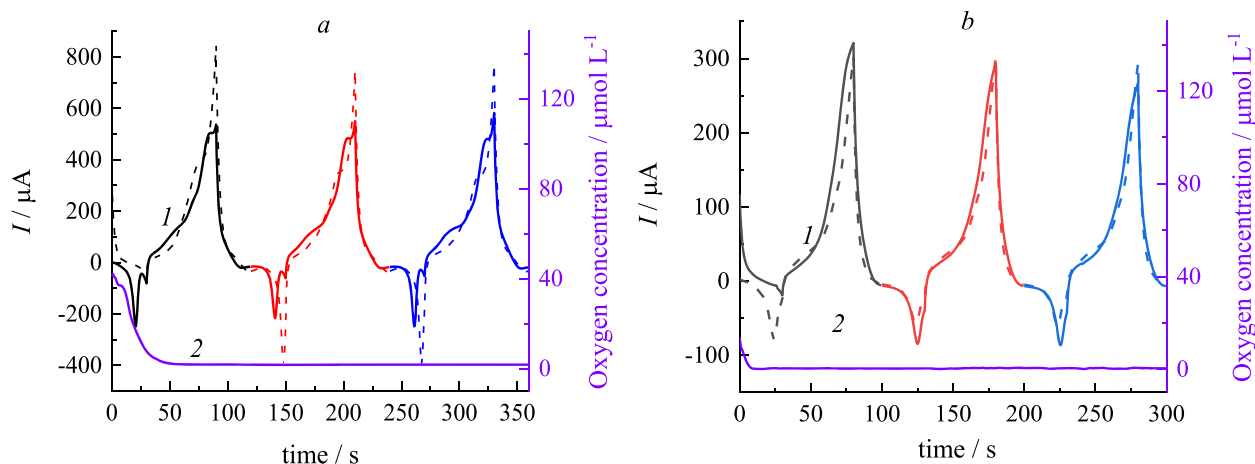
Fig. 8. Overlaid oxygen electrochemical responses recorded from Pd-ink modified SPE during CV (*1*) and results of simultaneous oxygen minisensor measurements (*2*) in HC medium, pH 12+100 mM glycerol. Polarization limit: *(a)* – 0.8 V, *(b)* – 0.6 V. Scan rate 20 mV/s. *Note*: various colors of curve *1* indicates the different cycles of CV (1st, 2nd, 3rd); dashed lines – current responses in a background solution, HC medium pH 12 (in the absence of glycerol), all potentials given *vs.* Ag/Ag$_2$O electrode.

Table 2.

Electroanalytical results[a] of glycerol quantification in HC fermentation medium at pH 12 on Pd-modified electrodes polarized from -0.4 V to 0.8 V[b] at 20 mV/s.

Functional layer	Calibration formula	R^2	Concentration of glycerol, mM[d]	RSD, %	Sensitivity, μA mM^{-1} cm^{-2}
Pd-NPs	$y^c = 0.39 \cdot x + 25.5$	0.999	65.58	1.18	0.195
Pd-ink	$y^c = 5.12 \cdot x + 281.6$	0.999	55.00	2.61	0.552
Hybrid Pd-ink/Pd-NPs	$y^c = 5.43 \cdot x + 325.4$	0.997	59.92	1.22	1.108

[a] typical CV plots and calibration curve are summarized in **ESI, Fig. S11** (shown for the hybrid electrode as a case study);.

[b] read-out at 0.6 V; anodic limit 0.8 V;.

[c] in standard addition approach y (μA) = 0, x – is the concentration of analyte, mM;.

[d] cells with OD = 5.1 obtained after 24 h of cultivation were removed from the medium by centrifugation prior to analysis. The remaining medium was used for the subsequent analysis.

for smaller analogues despite the opposite ECSA values found for these electrodes.

Notably, the obtained quantitative results were in line with GC–MS analysis conducted after derivatization following standard addition approach [51,52] of glycerol solutions. The concentration of glycerol was defined by GC–MS on the level of 60.2 mM with RSD 15.8 %, **ESI, Fig. S12**. In contrast, by Pd-based electrocatalysts glycerol was quantified in fermentation sample with RSD below 3 % (Table 2).

In summary, the proposed designs of the functional Pd layers of SPEs can be successfully applied for rapid measurements of glycerol concentration in fermentation samples without preliminary sample derivatization or separation.

4. Conclusion

In this study we tried to reveal and systemize key physicochemical parameters affecting the electrooxidation of glycerol at alkaline pH in model aqueous and real fermentation solutions. More specifically, during investigations it was found that the anodic polarization limit turns up an even more significant factor impacting electrochemical activity of the studied Pd-electrodes than their electroactive surface area (ECSA) (*1*). Surprisingly, the adsorption of glycerol appears to be not a

dominant factor in its total electrooxidation route as compared to hydroxyls (*2*).

By quantum-chemical simulations, the role of oxygen on the efficiency of glycerol electrooxidation was highlighted (*3*). The obtained calculations were further confirmed by experiments using the needle optical oxygen minisensor. Briefly, the deficit of dissolved oxygen suppressed the glycerol electrooxidation on Pd electrocatalysts at alkaline pH.

Moreover, Pd-electrodes with large particles (500 – 1000 nm, *e.g.,* Pd-ink or hybrid Pd-NPs/Pd-ink layers) were found to show weak interactions with oxygen and, hence, could be more active in glycerol oxidation reaction. In other words, the larger Pd-particles better catalyze glycerol oxidation (*4*).

The obtained knowledges were used to assist the controlled choice of Pd-electrodes for an efficient glycerol electrooxidation in complex fermentation media. The highest electroanalytical sensitivity for glycerol determination in both model buffered and a fermentation medium solution was reached using the hybrid Pd-ink/Pd-NPs-modified electrode. The performed recovery studies indicate that it is possible to determine glycerol in real samples, and the proposed methodology can be a valuable tool for practical glycerol analysis.

CRediT authorship contribution statement

Y.E. Silina: Writing – original draft, Validation, Methodology, Funding acquisition, Conceptualization. **E.V. Butyrskaya:** Validation, Software, Methodology, Investigation, Formal analysis. **M. Koch:** Writing – review & editing, Methodology, Investigation, Formal analysis. **C. Fink-Straube:** Methodology, Investigation, Formal analysis. **N. Korkmaz:** Validation, Software, Methodology, Investigation, Formal analysis. **M.G. Levchenko:** Methodology, Investigation, Formal analysis. **E.V. Zolotukhina:** Writing – review & editing, Visualization, Validation, Methodology, Data curation.

Declaration of competing interest

The authors declare that they have no known competing financial interests or personal relationships that could have appeared to influence the work reported in this paper.

Data availability

Data will be made available on request.

Supplementary materials

Supplementary material associated with this article can be found, in the online version, at doi:10.1016/j.electacta.2024.144479.

References

[1] J. Kuhn, H. Müller, D. Salzig, P. Czermak, A rapid method for an offline glycerol determination during microbial fermentation, Electron. J. Biotechnol. 18 (2015) 252–255, https://doi.org/10.1016/j.ejbt.2015.01.005.

[2] K. Pontius, D. Semenova, Y.E. Silina, K.V. Gernaey, H. Junicke, Automated electrochemical glucose biosensor platform as an efficient tool toward on-line fermentation monitoring: novel application approaches and insights, Front. Bioeng. Biotechnol. 8 (2020) 1–15, https://doi.org/10.3389/fbioe.2020.00436.

[3] M. Semkiv, K. Dmytruk, C. Abbas, A. Sibirny, Biotechnology of Glycerol Production and Conversion in Yeasts BT - Biotechnology of Yeasts and Filamentous Fungi, in: A.A. Sibirny (Ed.), Springer International Publishing, Cham, 2017: pp. 117–148. 10.1007/978-3-319-58829-2_5.

[4] Y. Zhou, Y. Shen, X. Luo, G. Liu, Y. Cao, Boosting activity and selectivity of glycerol oxidation over platinum–palladium–silver electrocatalysts via surface engineering, Nanoscale Advances 2 (2020) 3423–3430, https://doi.org/10.1039/D0NA00252F.

[5] P.A. Alaba, C.S. Lee, F. Abnisa, M.K. Aroua, P. Cognet, Y. Pérès, W.M.A. Wan Daud, A review of recent progress on electrocatalysts toward efficient glycerol electrooxidation, 2021. 10.1515/revce-2019-0013.

[6] T. Li, D.A. Harrington, An overview of glycerol electrooxidation mechanisms on Pt, Pd and Au, ChemSusChem. 14 (2021) 1472–1495, https://doi.org/10.1002/cssc.202002669.

[7] E. Antolini, Glycerol electro-oxidation in alkaline media and alkaline direct glycerol fuel cells, Catalysts 9 (2019), https://doi.org/10.3390/catal9120980.

[8] S.A. Kleinikova, M.G. Levchenko, A.B. Yalmaev, N.V. Talagaeva, N.N. Dremova, E.V. Gerasimova, E.V. Zolotukhina, Some features of alcohols electrooxidation process on Pd, Rh and PdRh catalysts, Electrochim. Acta 409 (2022) 139998, https://doi.org/10.1016/j.electacta.2022.139998.

[9] E.V. Gerasimova, S.A. Kleinikova, N.V. Talagaeva, K.V. Gor'kov, M.G. Levchenko, E.V. Zolotukhina, New insight on the study of electrocatalytic oxidation of methanol on some Pt group metals: important methodological aspects, Int. J. Hydrogen Energy 48 (2023) 34396–34409, https://doi.org/10.1016/j.ijhydene.2023.05.233.

[10] A. Nakova, M. Ilieva, T. Boijadjieva-Scherzer, V. Tsakova, Glycerol oxidation on Pd nanocatalysts obtained on PEDOT-coated graphite supports, Electrochim. Acta 306 (2019) 643–650, https://doi.org/10.1016/j.electacta.2019.03.151.

[11] H. Wang, L. Thia§, N. Li, X. Ge, Z. Liu, X. Wang, Pd nanoparticles on carbon nitride–graphene for the selective electro-oxidation of glycerol in alkaline solution, ACS Catal. 5 (2015) 3174–3180, https://doi.org/10.1021/acscatal.5b00183.

[12] R. Ivanov, A. Nakova, V. Tsakova, Glycerol oxidation at Pd nanocatalysts obtained through spontaneous metal deposition on carbon substrates, Electrochim. Acta 427 (2022) 140871, https://doi.org/10.1016/j.electacta.2022.140871.

[13] E. Habibi, H. Razmi, Glycerol electrooxidation on Pd, Pt and Au nanoparticles supported on carbon ceramic electrode in alkaline media, Int. J. Hydrogen Energy 37 (2012) 16800–16809, https://doi.org/10.1016/j.ijhydene.2012.08.127.

[14] M. Simões, S. Baranton, C. Coutanceau, Electro-oxidation of glycerol at Pd based nano-catalysts for an application in alkaline fuel cells for chemicals and energy cogeneration, Appl. Catal. B 93 (2010) 354–362, https://doi.org/10.1016/j.apcatb.2009.10.008.

[15] Y. Holade, C. Morais, K. Servat, T.W. Napporn, K.B. Kokoh, Toward the electrochemical valorization of glycerol: fourier transform infrared spectroscopic and chromatographic studies, ACS Catal. 3 (2013) 2403–2411, https://doi.org/10.1021/cs400559d.

[16] Y. Zhou, Y. Shen, Selective electro-oxidation of glycerol over Pd and Pt@Pd nanocubes, Electrochem. commun. 90 (2018) 106–110, https://doi.org/10.1016/j.elecom.2018.04.012.

[17] Z.-Y. Zhou, Q. Wang, J.-L. Lin, N. Tian, S.-G. Sun, In situ FTIR spectroscopic studies of electrooxidation of ethanol on Pd electrode in alkaline media, Electrochim. Acta 55 (2010) 7995–7999, https://doi.org/10.1016/j.electacta.2010.02.071.

[18] G. Cui, S. Song, P.K. Shen, A. Kowal, C. Bianchini, First-principles considerations on catalytic activity of Pd toward ethanol oxidation, J. Phys. Chem. C 113 (2009) 15639–15642, https://doi.org/10.1021/jp900924s.

[19] T. Sheng, W.-F. Lin, C. Hardacre, P. Hu, Role of water and adsorbed hydroxyls on ethanol electrochemistry on Pd: new mechanism, active centers, and energetics for direct ethanol fuel cell running in alkaline medium, J. Phys. Chem. C 118 (2014) 5762–5772, https://doi.org/10.1021/jp407978h.

[20] E.D. Wang, J.B. Xu, T.S. Zhao, Density functional theory studies of the structure sensitivity of ethanol oxidation on palladium surfaces, J. Phys. Chem. C 114 (2010) 10489–10497, https://doi.org/10.1021/jp101244t.

[21] B.D. Adams, A. Chen, The role of palladium in a hydrogen economy, Mater. Today 14 (2011) 282–289, https://doi.org/10.1016/S1369-7021(11)70143-2.

[22] L. Moumaneix, A. Rautakorpi, T. Kallio, Interactions between hydrogen and palladium nanoparticles: resolving adsorption and absorption contributions, ChemElectroChem 10 (2023) e202201109, https://doi.org/10.1002/celc.202201109.

[23] J. Campeggio, V. Volkov, M. Innocenti, W. Giurlani, C. Fontanesi, M. Zerbetto, M. Pagliai, A. Lavacchi, R. Chelli, Ethanol electro-oxidation reaction on the Pd (111) surface in alkaline media: insights from quantum and molecular mechanics, Phys. Chem. Chem. Phys. 24 (2022) 12569–12579, https://doi.org/10.1039/D2CP00909A.

[24] A. Pop, F. Manea, C. Radovan, D. Dascalu, N. Vaszilcsin, J. Schoonman, Non-enzymatic electrochemical detection of glycerol on boron-doped diamond electrode, Analyst 137 (2012) 641–647, https://doi.org/10.1039/C2AN15645H.

[25] E.V. Zolotukhina, E.V. Butyrskaya, M. Koch, P. Herbeck-Engel, M.G. Levchenko, Y.E. Silina, First principles of hydrazine electrooxidation at oxide-free and oxide-based palladium electrodes in complex media, Phys. Chem. Chem. Phys. (2023), https://doi.org/10.1039/D3CP00829K.

[26] Y.E. Silina, E.V. Zolotukhina, M. Koch, C. Fink-Straube, A tandem of GC-MS and electroanalysis for a rapid chemical profiling of bacterial extracellular matrix, Electroanalysis (2023) 1–16, https://doi.org/10.1002/elan.202300178.

[27] M.M. Francl, W.J. Pietro, W.J. Hehre, J.S. Binkley, M.S. Gordon, D.J. DeFrees, J.A. Pople, Self-consistent molecular orbital methods. XXIII. a polarization-type basis set for second-row elements, J. Chem. Phys. 77 (1982) 3654–3665, https://doi.org/10.1063/1.444267.

[28] C.M. Lousada, A.J. Johansson, T. Brinck, M. Jonsson, Reactivity of metal oxide clusters with hydrogen peroxide and water – a DFT study evaluating the performance of different exchange–correlation functionals, Phys. Chem. Chem. Phys. 15 (2013) 5539–5552, https://doi.org/10.1039/C3CP44559C.

[29] G.I. Cárdenas-Jirón, C. Paredes-García, D. Venegas-Yazigi, J.H. Zagal, M. Páez, J. Costamagna, Theoretical modeling of the oxidation of hydrazine by iron(II) phthalocyanine in the gas phase. influence of the metal character, J. Phys. Chem. A 110 (2006) 11870–11875, https://doi.org/10.1021/jp060647r.

[30] N.A. Al Abass, G. Denuault, D. Pletcher, The unexpected activity of Pd nanoparticles prepared using a non-ionic surfactant template, Phys. Chem. Chem. Phys. 16 (2014) 4892–4899, https://doi.org/10.1039/C3CP54531H.

[31] S.-S. Li, Y.-Y. Hu, J.-J. Feng, Z.-Y. Lv, J.-R. Chen, A.-J. Wang, Rapid room-temperature synthesis of Pd nanodendrites on reduced graphene oxide for catalytic oxidation of ethylene glycol and glycerol, Int. J. Hydrogen Energy 39 (2014) 3730–3738, https://doi.org/10.1016/j.ijhydene.2013.12.159.

[32] X. Zhang, P.K. Shen, Glycerol electrooxidation on highly active Pd supported carbide/C aerogel composites catalysts, Int. J. Hydrogen Energy 38 (2013) 2257–2262, https://doi.org/10.1016/j.ijhydene.2012.11.119.

[33] B. Rezaei, E. Havakeshian, A.A. Ensafi, Fabrication of a porous Pd film on nanoporous stainless steel using galvanic replacement as a novel electrocatalyst/electrode design for glycerol oxidation, Electrochim. Acta 136 (2014) 89–96, https://doi.org/10.1016/j.electacta.2014.05.041.

[34] S. Dash, N. Munichandraiah, Electrocatalytic oxidation of 1,2-propanediol on electrodeposited Pd–poly(3,4-ethylenedioxythiophene) nanodendrite films in alkaline medium, Electrochim. Acta 80 (2012) 68–76, https://doi.org/10.1016/j.electacta.2012.06.130.

[35] O.O. Fashedemi, K.I. Ozoemena, Comparative electrocatalytic oxidation of ethanol, ethylene glycol and glycerol in alkaline medium at Pd-decorated FeCo@Fe/C core-shell nanocatalysts, Electrochim. Acta 128 (2014) 279–286, https://doi.org/10.1016/j.electacta.2013.10.194.

[36] G.G. Honório, J.N. da Cunha, K.L. dos Santos Castro Assis, P.F. de Aguiar, D.F. de Andrade, C.G. de Souza, L.A. d'Avila, B.S. Archanjo, C.A. Achete, R.N.C. Pradelle, F. Turkovics, R.S. Neto, E. D'Elia, Free glycerol determination in biodiesel samples using palladium nanoparticles modified glassy carbon electrode associated with solid phase extraction, J. Solid State Electrochem. 23 (2019) 3057–3066, https://doi.org/10.1007/s10008-019-04387-2.

[37] R.P. Buck, L.R. Griffith, Voltammetric and Chronopotentiometric Study of the Anodic Oxidation of Methanol, Formaldehyde, and Formic Acid, J. Electrochem. Soc. 109 (1962) 1005, https://doi.org/10.1149/1.2425226.

[38] S.C.S. Lai, S.E.F. Kleijn, F.T.Z. Öztürk, V.C. van Rees Vellinga, J. Koning, P. Rodriguez, M.T.M. Koper, Effects of electrolyte pH and composition on the ethanol electro-oxidation reaction, Catal. Today 154 (2010) 92–104, https://doi.org/10.1016/j.cattod.2010.01.060.

[39] K.V. Gor'kov, N.V. Talagaeva, S.A. Kleinikova, N.N. Dremova, M.A. Vorotyntsev, E.V. Zolotukhina, Palladium-polypyrrole composites as prospective catalysts for formaldehyde electrooxidation in alkaline solutions, Electrochim. Acta 345 (2020) 136164, https://doi.org/10.1016/j.electacta.2020.136164.

[40] Ermete Antolini, Glycerol electro-oxidation in alkaline media and alkaline direct glycerol fuel cells, Catalysts (2019) 980.

[41] I.U. of P. and A. Chemistry, E.P. Serjeant, B. Dempsey, I.U. of P. and A.C.C. on E. Data, Ionisation Constants of Organic Acids in Aqueous Solution, Pergamon Press Oxford, Oxford SE - xi, 1979, p. 989, pages ; 28 cmLK -, https://worldcat.org/title/4494248.

[42] C.A. Lewis, R. Wolfenden, Influence of pressure on the equilibrium of hydration of aliphatic aldehydes, J. Am. Chem. Soc. 95 (1973) 6685–6688, https://doi.org/10.1021/ja00801a026.

[43] S.J. Reynolds, D.W. Yates, C.I. Pogson, Dihydroxyacetone phosphate. its structure and reactivity with α-glycerophosphate dehydrogenase, aldolase and triose

phosphate isomerase and some possible metabolic implications, Biochem. J. 122 (1971) 285–297, https://doi.org/10.1042/bj1220285.

[44] S.A.N.M. Rahim, C.S. Lee, F. Abnisa, M.K. Aroua, W.A.W. Daud, P. Cognet, Y. Pérès, A review of recent developments on kinetics parameters for glycerol electrochemical conversion – A by-product of biodiesel, Sci. Total Environ. 705 (2020) 135137, https://doi.org/10.1016/j.scitotenv.2019.135137.

[45] A. Plauck, E.E. Stangland, J.A. Dumesic, M. Mavrikakis, Active sites and mechanisms for H_2O_2 decomposition over Pd catalysts, Proc. Natl. Acad. Sci. U.S.A. 113 (2016) E1973–E1982, https://doi.org/10.1073/pnas.1602172113.

[46] D. Semenova, Y.E. Silina, M. Koch, L. Micheli, A. Zubov, K.V. Gernaey, Sensors for biosensors: a novel tandem monitoring in a droplet towards efficient screening of robust design and optimal operating conditions, Analyst (2019), https://doi.org/10.1039/c8an02261e.

[47] W.B. Gleason, R. Barker, Oxidation of pentoses in alkaline solution, Can. J. Chem. 49 (1971) 1425–1432, https://doi.org/10.1139/v71-234.

[48] J. Uranga, J.I. Mujika, R. Grande-Aztatzi, J.M. Matxain, Oxidation of acid, base, and amide side-chain amino acid derivatives via hydroxyl radical, J. Phys. Chem. B 122 (2018) 4956–4971, https://doi.org/10.1021/acs.jpcb.7b12450.

[49] O. Sarkar, U. Rova, P. Christakopoulos, L. Matsakas, Influence of initial uncontrolled pH on acidogenic fermentation of brewery spent grains to biohydrogen and volatile fatty acids production: Optimization and scale-up, Bioresource Technology 319 (2021) 124233, https://doi.org/10.1016/j.biortech.2020.124233.

[50] J.R. Clamp, L. Hough, The periodate oxidation of amino acids with reference to studies on glycoproteins, Biochem. J. 94 (1965) 17–24, https://doi.org/10.1042/bj0940017.

[51] M. Gergov, T. Nenonen, I. Ojanperä, R.A. Ketola, Compensation of matrix effects in a standard addition method for metformin in postmortem blood using liquid chromatography–electrospray–tandem mass spectrometry, J. Anal. Toxicol. 39 (2015) 359–364, https://doi.org/10.1093/jat/bkv020.

[52] M.P. Juhascik, A.J. Jenkins, Comparison of tissue homogenate analytical results with and without standard addition, J. Anal. Toxicol. 35 (2011) 179–182, https://doi.org/10.1093/anatox/35.3.179.

[53] M. Bader, A systematic approach to standard addition methods in instrumental analysis, J. Chem. Educ. 57 (1980) 703, https://doi.org/10.1021/ed057p703.